Journal of Magnetism and Magnetic Materials 407 (2016) 341–347

Contents lists available at ScienceDirect

Journal of Magnetism and Magnetic Materials

journal homepage: www.elsevier.com/locate/jmmm

Spin-1 $J_1 - J_2 - J_3$ ferromagnetic Heisenberg model with an easy-plane crystal field on the cubic lattice: A bosonic approach

D.C. Carvalho [a,b,*], A.S.T. Pires [b], L.A.S. Mól [b]

[a] Instituto Federal do Norte de Minas Gerais, Fazenda Varginha, km 02. Rodovia Salinas/Taiobeiras, CEP 39560-000, Salinas, MG, Brazil
[b] Departamento de Física, Instituto de Ciências Exatas, Universidade Federal de Minas Gerais, C.P. 702, 30123-970 Belo Horizonte, MG, Brazil

ARTICLE INFO

Article history:
Received 7 October 2015
Received in revised form
5 January 2016
Accepted 1 February 2016

Keywords:
Quantum phase transition
Bond-operator formalism
Quantum spin liquid
Frustrated Heisenberg model
Single-ion anisotropy

ABSTRACT

We examine the phase diagram of the spin-1 $J_1 - J_2 - J_3$ ferromagnetic Heisenberg model with an easy-plane crystal field on the cubic lattice, in which J_1 is the ferromagnetic exchange interaction between nearest neighbors, J_2 is the antiferromagnetic exchange interaction between next-nearest neighbors and J_3 is the antiferromagnetic exchange interaction between next-next-nearest neighbors. Using the bond-operator formalism, we investigate the phase transitions between the disordered paramagnetic phase and the ordered ones. We show that the nature of the quantum phase transitions changes as the frustration parameters ($\frac{J_2}{J_1}$, $\frac{J_3}{J_1}$) are varied. The zero-temperature phase diagram exhibits second- and first-order transitions, depending on the energy gap behavior. Remarkably, we find a disordered nonmagnetic phase, even in the absence of a crystal field, which is suggested to be a quantum spin liquid candidate. We also depict the phase diagram at finite temperature for some values of crystal field and frustration parameters.

1. Introduction

The investigation of frustrated quantum spin models has attracted a lot of attention since Anderson proposed theoretically the existence of a non-magnetic ground state in a triangular lattice [1]. Such a disordered state is known as a quantum spin liquid. From a theoretical point of view, the association between frustration and quantum fluctuations is believed to give rise to this novel quantum phase [2]. While quantum fluctuations are introduced by the non-commutativity of quantum mechanics spin operators, frustration arises either from competition between different interactions, e.g. ferromagnetic and antiferromagnetic couplings [3,4], or from geometry of the lattice, e.g. spins that interact via antiferromagnetic coupling on several lattices [5,6].

As a result, spin models that have both strong quantum fluctuations and frustration are candidates to exhibit quantum spin liquid phase. In fact, most of theoretical researches have been concentrated on spin-1/2 models in one- and two-dimensional lattices, since, in these cases, quantum fluctuations are enhanced (see, for example, Refs. [7–9]). However, three-dimensional compounds have recently been suggested to present a quantum spin liquid phase [10–12], which turns our attention to the theoretical investigation of three-dimensional models.

On the other hand, the discovery of spin-1 compounds has led to a lot of experimental and theoretical studies of the effect of single-ion anisotropy. In fact, there has been recently an interest in the study of quantum phase transitions in spin-1 magnets with strong single-ion anisotropy (see, for example, Ref. [13] and references there in). These systems become quantum paramagnets for sufficiently high values of the easy-plane single-ion anisotropy, which is purely a quantum effect without a counterpart in the classical models.

In addition, a quantum spin liquid phase has recently been discovered in the compound $Ba_3NiSb_2O_9$ [14,15], which behaves effectively as a spin-1 system. This also motivates the theoretical investigation of spin-liquid behavior in spin-1 models.

In this paper, we study the phase diagram of spin-1 $J_1 - J_2 - J_3$ ferromagnetic Heisenberg model with an easy-plane crystal field on the cubic lattice, which is defined by the following Hamiltonian:

$$\mathcal{H} = -\frac{J_1}{2}\sum_{\vec{r},\vec{\delta}_1}\vec{S}_{\vec{r}}\cdot\vec{S}_{\vec{r}+\vec{\delta}_1} + \frac{J_2}{2}\sum_{\vec{r},\vec{\delta}_2}\vec{S}_{\vec{r}}\cdot\vec{S}_{\vec{r}+\vec{\delta}_2} + \frac{J_3}{2}\sum_{\vec{r},\vec{\delta}_3}\vec{S}_{\vec{r}}\cdot\vec{S}_{\vec{r}+\vec{\delta}_3} + D\sum_{\vec{r}}\left(S^z_{\vec{r}}\right)^2, \quad (1)$$

where $\sum_{\vec{r},\vec{\delta}_i}$ sums over the first neighbors for $i=1$, over the second neighbors for $i=2$, and over the third neighbors for $i=3$. J_1 is the ferromagnetic exchange interaction between nearest neighbors, J_2

* Corresponding author at: Instituto Federal do Norte de Minas Gerais, Fazenda Varginha, km 02. Rodovia Salinas/Taiobeiras, CEP 39560-000, Salinas, MG, Brazil.

http://dx.doi.org/10.1016/j.jmmm.2016.02.001
0304-8853/

is the antiferromagnetic exchange interaction between next-nearest neighbors and J_3 is the antiferromagnetic exchange interaction between next-next-nearest neighbors. The last sum is over the total number of sites on the cubic lattice, N, and $D > 0$ is the easy-plane crystal field that gives rise to a single-ion anisotropy. $\vec{S}_{\vec{r}}$ is the spin operator at site $\vec{r}$ with $S^z_{\vec{r}}$ taking the eigenvalues −1, 0, 1.

To the best of our knowledge, the above Hamiltonian has not been examined yet. Only its counterpart model with all antiferromagnetic couplings (J_1, J_2, J_3) has been treated in Ref. [16], which is less interesting because in this case, J_1 and J_3 does not compete with each other. Thus the present Hamiltonian (1) is much more suitable to seek quantum spin liquid candidates. In addition, compounds with both ferromagnetic and antiferromagnetic exchange interactions have been reported in the literature (see Ref. [3] and references therein), which indicates that the present model with competitive interactions may be interesting not only from a theoretical perspective.

In order to study the phase diagram of this frustrated Heisenberg model, we use an analytical approach that has been successfully employed to describe transitions from a gapped to a gapless phase, namely bond-operator formalism [17–20]. In a few words, within the framework of the bond-operator theory, the spin Hamiltonian is mapped into a Hamiltonian of non-interacting bosons, and phase transitions are located when the energy gap vanishes.

It should be pointed out that, in general, analytical approaches are more adequate to treat three-dimensional frustrated quantum spin systems than numerical methods, by reason of the limited amount of computational power. In particular, it is well known that quantum Monte Carlo suffers from the minus-sign problem which restricts its applicability: only non-frustrated quantum spin systems [21].

The present paper is organized as follows. In the next section we describe the bond-operator formalism and how phase transitions are characterized within this framework. In Section 3, we show the results for the phase diagrams at finite temperature and at absolute zero as well. We also discuss the physical meaning of the obtained results. We close with some concluding remarks.

2. Bond-operator formalism

We employ the bond-operator formalism in order to investigate the phase diagram of the present model. This procedure was originally devised by Sachdev and Bhatt [22], for spin-1/2, and generalized by Wang et al. [17,23], for spin-1, some years later. To begin we describe the method briefly below.

For spin-1, by introducing three boson operators, it is possible to represent the three eigenstates of S^z as follows:

$$|1\rangle = u^\dagger|v\rangle,$$

$$|0\rangle = t_z^\dagger|v\rangle,$$

$$|-1\rangle = d^\dagger|v\rangle, \tag{2}$$

where $|v\rangle$ is the vacuum state from which bosons are created. These boson operators must also obey the local constraint

$$u^\dagger u + d^\dagger d + t_z^\dagger t_z = \hat{1} \tag{3}$$

in order to keep the dimension of the local Hilbert space invariant.

Now, we can write the spin operators S^x, S^y and S^z in terms of these bosons operators:

$$S^x = \frac{1}{\sqrt{2}}[(u^\dagger + d^\dagger)t_z + t_z^\dagger(u + d)],$$

$$S^y = \frac{1}{\sqrt{2}\,i}[(u^\dagger - d^\dagger)t_z - t_z^\dagger(u - d)],$$

$$S^z = u^\dagger u - d^\dagger d. \tag{4}$$

Substituting the above relations into Eq. (1), the Hamiltonian can be rewritten as a sum of four components

$$\mathcal{H} = \mathcal{H}_1 + \mathcal{H}_2 + \mathcal{H}_3 + \mathcal{H}_4, \tag{5}$$

with

$$\mathcal{H}_1 = -\frac{J_1}{2}\sum_{\vec{r},\vec{\delta}_1}\Big\{\Big[\Big(d^\dagger_{\vec{r}}d_{\vec{r}+\vec{\delta}_1} + u^\dagger_{\vec{r}}u_{\vec{r}+\vec{\delta}_1}\Big)t_{z,\vec{r}}t^\dagger_{z,\vec{r}+\vec{\delta}_1} + \Big(u^\dagger_{\vec{r}}d^\dagger_{\vec{r}+\vec{\delta}_1} + d^\dagger_{\vec{r}}u^\dagger_{\vec{r}+\vec{\delta}_1}\Big)t_{z,\vec{r}}t_{z,\vec{r}+\vec{\delta}_1} + H.\,c.\Big] + \Big(u^\dagger_{\vec{r}}u_{\vec{r}} - d^\dagger_{\vec{r}}d_{\vec{r}}\Big)\Big(u^\dagger_{\vec{r}+\vec{\delta}_1}u_{\vec{r}+\vec{\delta}_1} - d^\dagger_{\vec{r}+\vec{\delta}_1}d_{\vec{r}+\vec{\delta}_1}\Big)\Big\},$$

$$\mathcal{H}_2 = \frac{J_2}{2}\sum_{\vec{r},\vec{\delta}_2}\Big\{\Big[\Big(d^\dagger_{\vec{r}}d_{\vec{r}+\vec{\delta}_2} + u^\dagger_{\vec{r}}u_{\vec{r}+\vec{\delta}_2}\Big)t_{z,\vec{r}}t^\dagger_{z,\vec{r}+\vec{\delta}_2} + \Big(u^\dagger_{\vec{r}}d^\dagger_{\vec{r}+\vec{\delta}_2} + d^\dagger_{\vec{r}}u^\dagger_{\vec{r}+\vec{\delta}_2}\Big)t_{z,\vec{r}}t_{z,\vec{r}+\vec{\delta}_2} + H.\,c.\Big] + \Big(u^\dagger_{\vec{r}}u_{\vec{r}} - d^\dagger_{\vec{r}}d_{\vec{r}}\Big)\Big(u^\dagger_{\vec{r}+\vec{\delta}_2}u_{\vec{r}+\vec{\delta}_2} - d^\dagger_{\vec{r}+\vec{\delta}_2}d_{\vec{r}+\vec{\delta}_2}\Big)\Big\},$$

$$\mathcal{H}_3 = \frac{J_3}{2}\sum_{\vec{r},\vec{\delta}_3}\Big\{\Big[\Big(d^\dagger_{\vec{r}}d_{\vec{r}+\vec{\delta}_3} + u^\dagger_{\vec{r}}u_{\vec{r}+\vec{\delta}_3}\Big)t_{z,\vec{r}}t^\dagger_{z,\vec{r}+\vec{\delta}_3} + \Big(u^\dagger_{\vec{r}}d^\dagger_{\vec{r}+\vec{\delta}_3} + d^\dagger_{\vec{r}}u^\dagger_{\vec{r}+\vec{\delta}_3}\Big)t_{z,\vec{r}}t_{z,\vec{r}+\vec{\delta}_3} + H.\,c.\Big] + \Big(u^\dagger_{\vec{r}}u_{\vec{r}} - d^\dagger_{\vec{r}}d_{\vec{r}}\Big)\Big(u^\dagger_{\vec{r}+\vec{\delta}_3}u_{\vec{r}+\vec{\delta}_3} - d^\dagger_{\vec{r}+\vec{\delta}_3}d_{\vec{r}+\vec{\delta}_3}\Big)\Big\},$$

$$\mathcal{H}_4 = D\sum_{\vec{r}}\Big(u^\dagger_{\vec{r}}u_{\vec{r}} + d^\dagger_{\vec{r}}d_{\vec{r}}\Big) - \sum_{\vec{r}}\mu_{\vec{r}}\Big(u^\dagger_{\vec{r}}u_{\vec{r}} + d^\dagger_{\vec{r}}d_{\vec{r}} + t^\dagger_{z,\vec{r}}t_{z,\vec{r}} - 1\Big), \tag{6}$$

where a temperature-dependent chemical potential, $\mu_{\vec{r}}$, has been introduced to guarantee the single-site occupancy, and *H.c.* means Hermitian conjugate.

In order to treat the above Hamiltonian, it is necessary to make some approximations at mean-field level:

- Firstly, the condensation of t_z bosons is required, i.e. $\langle t_z\rangle = \langle t_z^\dagger\rangle = t$. This approach, as shown by Zhang et al. [13], is very accurate to treat phases where $\langle S^z\rangle = 0$.
- Secondly, the four-operator terms of the Hamiltonian components ($\mathcal{H}_1$, $\mathcal{H}_2$ and $\mathcal{H}_3$) are decoupled into product of two operators, as done in Ref. [17]. For the component $\mathcal{H}_1$, for example, one obtains

$$\begin{aligned}\Big(u^\dagger_{\vec{r}}u_{\vec{r}} - d^\dagger_{\vec{r}}d_{\vec{r}}\Big)\Big(u^\dagger_{\vec{r}+\vec{\delta}_1}u_{\vec{r}+\vec{\delta}_1} - d^\dagger_{\vec{r}+\vec{\delta}_1}d_{\vec{r}+\vec{\delta}_1}\Big) &\approx \tfrac{1}{2}\big(1-t^2\big)\Big(u^\dagger_{\vec{r}}u_{\vec{r}} + u^\dagger_{\vec{r}+\vec{\delta}_1}u_{\vec{r}+\vec{\delta}_1}\Big) + \tfrac{1}{2}\big(1-t^2\big)\Big(d^\dagger_{\vec{r}}d_{\vec{r}} + d^\dagger_{\vec{r}+\vec{\delta}_1}d_{\vec{r}+\vec{\delta}_1}\Big)\\ &\quad - p_1\Big(u_{\vec{r}}d_{\vec{r}+\vec{\delta}_1} + d_{\vec{r}}u_{\vec{r}+\vec{\delta}_1} + H.\,c.\Big) - \tfrac{1}{2}(1-t^2)^2 + 2p_1^2,\end{aligned} \tag{7}$$

where $p_1 = \Big\langle d^\dagger_{\vec{r}}u^\dagger_{\vec{r}+\vec{\delta}_1}\Big\rangle = \Big\langle d_{\vec{r}}u_{\vec{r}+\vec{\delta}_1}\Big\rangle$. Similarly, one gets $p_2 = \Big\langle d^\dagger_{\vec{r}}u^\dagger_{\vec{r}+\vec{\delta}_2}\Big\rangle = \Big\langle d_{\vec{r}}u_{\vec{r}+\vec{\delta}_2}\Big\rangle$ and $p_3 = \Big\langle d^\dagger_{\vec{r}}u^\dagger_{\vec{r}+\vec{\delta}_3}\Big\rangle = \Big\langle d_{\vec{r}}u_{\vec{r}+\vec{\delta}_3}\Big\rangle$, for components $\mathcal{H}_2$ and $\mathcal{H}_3$, respectively.

- Lastly, the local constraint in Eq. (3) is replaced by a global constraint, that is, we assume that μ is site-independent, ignoring its fluctuations. A discussion about this approximation is presented in [24].

As a result, we arrive at a quadratic Hamiltonian involving boson operators. The next step in diagonalizing it is to take advantage of translational invariance by using Fourier transformed operators

$$d_{\vec{r}} = \frac{1}{\sqrt{N}} \sum_{\vec{k}} e^{-i\vec{k}\cdot\vec{r}} d_{\vec{k}}, \tag{8}$$

$$d^{\dagger}_{\vec{r}} = \frac{1}{\sqrt{N}} \sum_{\vec{k}} e^{i\vec{k}\cdot\vec{r}} d^{\dagger}_{\vec{k}}, \tag{9}$$

$$u_{\vec{r}} = \frac{1}{\sqrt{N}} \sum_{\vec{k}} e^{-i\vec{k}\cdot\vec{r}} u_{\vec{k}}, \tag{10}$$

$$u^{\dagger}_{\vec{r}} = \frac{1}{\sqrt{N}} \sum_{\vec{k}} e^{i\vec{k}\cdot\vec{r}} u^{\dagger}_{\vec{k}}. \tag{11}$$

However, this is not sufficient to diagonalize completely the Hamiltonian. Hence, we make use of a linear combination of Fourier transformed operators

$$\begin{aligned} \alpha_{\vec{k}} &= \chi_k u_{\vec{k}} + \rho_k d^{\dagger}_{-\vec{k}}, \\ \beta_{\vec{k}} &= \chi_k d_{-\vec{k}} + \rho_k u^{\dagger}_{\vec{k}}, \end{aligned} \tag{12}$$

provided that $\chi_k^2 - \rho_k^2 = 1$. This is known as Bogoliubov transformation.

Finally, we write the diagonal form of the Hamiltonian

$$\mathcal{H} = \sum_{\vec{k}} \omega_k \left(\alpha^{\dagger}_{\vec{k}} \alpha_{\vec{k}} + \beta^{\dagger}_{\vec{k}} \beta_{\vec{k}} \right) + \sum_{\vec{k}} (\omega_k - \Lambda_k) + C, \tag{13}$$

where

$$\omega_k = \sqrt{\Lambda_k^2 - \Delta_k^2}, \tag{14}$$

$$\Lambda_k = \frac{1}{2}\left(1 - t^2\right)\left(- z_1 + \eta z_2 + \alpha z_3\right) + g(k)t^2 + D - \mu, \tag{15}$$

$$\Delta_k = g(k)t^2 - F(k), \tag{16}$$

$$g(k) = - z_1\gamma_{k_1} + \eta z_2\gamma_{k_2} + \alpha z_3\gamma_{k_3}, \tag{17}$$

$$F(k) = - z_1\gamma_{k_1}p_1 + \eta z_2\gamma_{k_2}p_2 + \alpha z_3\gamma_{k_3}p_3, \tag{18}$$

$$\gamma_{k_1} = \frac{1}{3}\left(\cos k_x + \cos k_y + \cos k_z\right), \tag{19}$$

$$\gamma_{k_2} = \frac{1}{3}\left(\cos k_x \cos k_y + \cos k_x \cos k_z + \cos k_y \cos k_z\right), \tag{20}$$

$$\gamma_{k_3} = \cos k_x \cos k_y \cos k_z, \tag{21}$$

$$\begin{aligned} C = {} & \frac{N(1 - t^2)^2}{4}\left(z_1 - \eta z_2 - \alpha z_3\right) + N\mu(1 - t^2) \\ & + N\left(- z_1p_1^2 + \eta z_2p_2^2 + \alpha z_3p_3^2\right). \end{aligned} \tag{22}$$

Two frustration parameters have been defined, namely $\eta = \frac{J_2}{J_1}$ and $\alpha = \frac{J_3}{J_1}$, and we have fixed $J_1 = 1$.

We can derive the energy of the ground state from the Hamiltonian of non-interacting bosons (13) by setting $\alpha^{\dagger}_{\vec{k}}\alpha_{\vec{k}} = \beta^{\dagger}_{\vec{k}}\beta_{\vec{k}} = 0$, since these operators count the number of bosons (excitations). Thus,

$$E_0 = C + \sum_{\vec{k}} (\omega_k - \Lambda_k). \tag{23}$$

It is also straightforward to obtain the Gibbs free energy

$$G = E_0 - \frac{2}{\beta} \sum_{\vec{k}} \ln[1 + n(\omega_k)], \tag{24}$$

where

$$n(\omega_k) = \frac{1}{e^{\beta\omega_k} - 1} \tag{25}$$

and $\beta = \frac{1}{k_BT}$ is the Boltzmann factor.

By minimizing the Gibbs free energy, we obtain a set of coupled equations from which the phase diagram of the model can be examined:

$$2 - t^2 = \frac{1}{N} \sum_{\vec{k}} \frac{\Lambda_k}{\omega_k} \coth\left(\frac{\beta\omega_k}{2}\right), \tag{26}$$

$$\mu = \frac{1}{N} \sum_{\vec{k}} \frac{\Lambda_k - \Delta_k}{\omega_k} g(k) \coth\left(\frac{\beta\omega_k}{2}\right), \tag{27}$$

$$p_i = - \frac{1}{2N} \sum_{\vec{k}} \frac{\Delta_k}{\omega_k}\gamma_{k_i} \coth\left(\frac{\beta\omega_k}{2}\right), \tag{28}$$

with $i = 1, 2, 3$.

Taking the continuum limit, the summation over $\vec{k}$ can be replaced by a triple integral, then these integrals are solved numerically by using the Gauss–Legendre method. We also apply the Newton–Raphson technique for solving these coupled equations.

2.1. Phase transitions

The classical version of the Hamiltonian (1) with $D=0$ has two ordered phases at absolute zero:

(i) A ferromagnetic phase (F) characterized by $\vec{k}_F = (0, 0, 0)$;
(ii) A collinear antiferromagnetic phase (CAF) characterized by $\vec{k}_{CAF} = (0, 0, \pi)$ or $\vec{k}_{CAF} = (0, \pi, 0)$ or $\vec{k}_{CAF} = (\pi, 0, 0)$.

It should be mentioned that in contrast to the classical $J_1 - J_2 - J_3$ antiferromagnetic Heisenberg model, the collinear antiferromagnetic phase with $\vec{k} = (0, \pi, \pi)$ is never stable in its ferromagnetic counterpart.

In order to verify the presence of these ordered phases in the

quantum Hamiltonian (1), we must analyze the energy gap for both phases F and CAF. According to the bond-operator formalism, phase transitions are obtained from the gapped phase (disordered) to the gapless phase (ordered) when the gap closes at the critical point.

For the F order, the boson modes become gapless at $\vec{k}_F$ and therefore $\omega_{\vec{k}_F} = 0$, which characterizes a phase transition between the disordered paramagnetic phase and the ferromagnetic phase. For the CAF order, the energy gap goes to zero at $\vec{k}_{CAF}$, then $\omega_{\vec{k}_{CAF}} = 0$, which characterizes a phase transition between the disordered paramagnetic phase and the collinear antiferromagnetic phase.

3. Results and discussion

In this section, we show numerical results obtained by solving the coupled equations ((26)–(28)) in the continuum limit. Phase diagrams at zero temperature as well as at finite temperature are analyzed as a function of the parameters of the Hamiltonian (1). Before starting the discussion, we remind the reader about the notation used herein: $\eta = \frac{J_2}{J_1}$ and $\alpha = \frac{J_3}{J_1}$.

3.1. Quantum phase diagram (T=0)

Fig. 1 shows the quantum phase diagram for $\alpha = 0$. One notes the presence of two ordered phases below the critical lines, namely F and CAF. For $0 \le \eta < 0.227$, the ferromagnetic phase is stable, while for $0.239 < \eta \le 1$, the collinear antiferromagnetic phase is stable. A remarkable finding is a narrow nonmagnetic phase between F and CAF phases along η-axis, for $0.227 \le \eta \le 0.239$, which is clearly depicted in the inset. Such a gapped phase, which is absent in the corresponding classical model, is a quantum spin liquid candidate.

It should be pointed out that the classical ground state of the present model with $D=0$ exhibits a transition between F and CAF phases for $\eta_{classical} = 0.25$ at $\alpha = 0$. Hence, one notes from Fig. 1 that when the quantum nature of the frustrated Heisenberg model is taken into account, the CAF phase is slightly enhanced while the F phase is weakened, and besides, a quantum nonmagnetic phase emerges between these phases.

Thus, our results indicate that even a three-dimensional model is able to host a quantum spin liquid phase, despite the fact that quantum fluctuations decrease with the increase of lattice dimensionality. Recently, a quantum spin liquid phase candidate has also been suggested on the cubic lattice for the spin-1/2 $J_1 - J_2 - J_3$ antiferromagnetic Heisenberg model by using the variational cluster approach [25], which corroborates our finding.

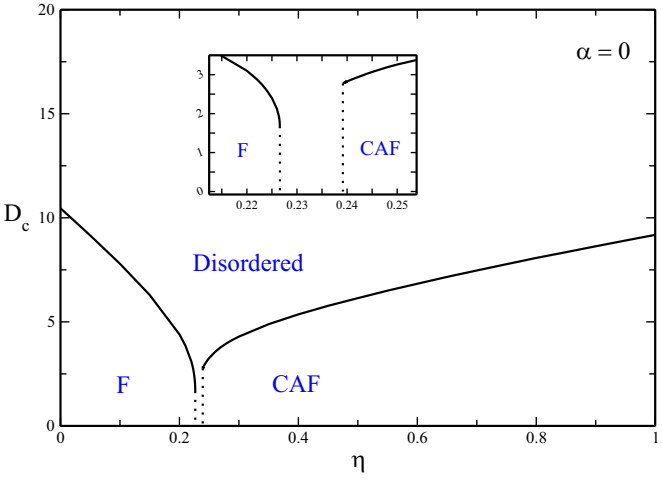

Fig. 1. Critical crystal field, D_c, as a function of the frustration parameter, η, at zero temperature, for $\alpha = 0$. The continuous lines refer to second-order quantum phase transitions, and the dotted lines refer to first-order ones. The inset shows the low crystal field region on a finer scale.

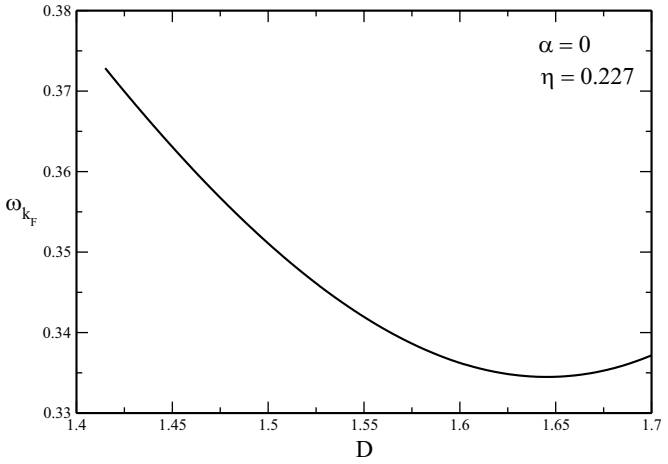

Fig. 2. The energy gap of the ferromagnetic phase, $\omega_{\vec{k}_F}$, as a function of the crystal field, D, at zero temperature, for $\alpha = 0$ and $\eta = 0.227$.

One can also see that the nature of the phase transitions varies with η. For $\eta = 0.227$ and $\eta = 0.239$, the energy gap does not vanish continuously, as one would expect at a critical point, by contrast, it passes through a finite minimal value. This is shown in Fig. 2 for $\eta = 0.227$. From $D=1.7$, we see clearly that the energy gap, $\omega_{\vec{k}_F}$, decreases with decreasing D, passes through a minimum, and then increases. Hence, we believe that the model undergoes first-order transitions for those values of η.

It is also worth analyzing the effect of the crystal field on the stability of the ordered phases. Note that the critical crystal field, D_c, for the F phase, decreases with increasing η, while for the CAF phase D_c increases. This can be understood as a result of the frustration that destroys the ferromagnetic order and favors the collinear antiferromagnetic one.

A similar phase diagram is obtained by letting $\alpha = 0.1$. As shown in Fig. 3, when we include the third-neighbor coupling, J_3, the ordered phases, F and CAF, are still present as well as the magnetically disordered one. However, the J_3 interaction reduces the F phase and increases the CAF order. Considering $D < D_c$, the F phase is stable for $0 \le \eta < 0.127$, while CAF phase is stable for $0.137 < \eta \le 1$.

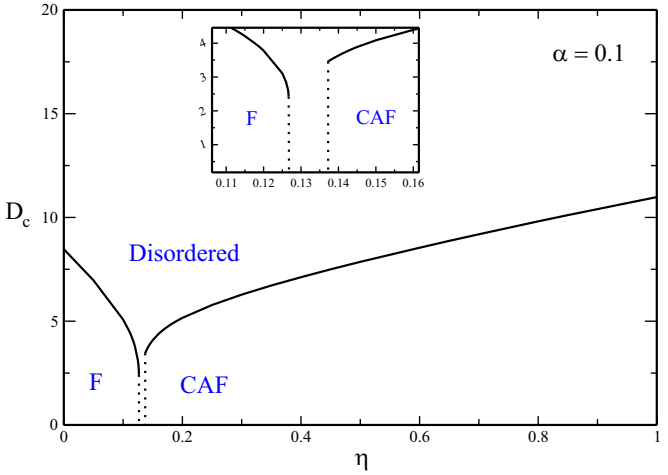

Fig. 3. The same as Fig. 1 for $\alpha = 0.1$.

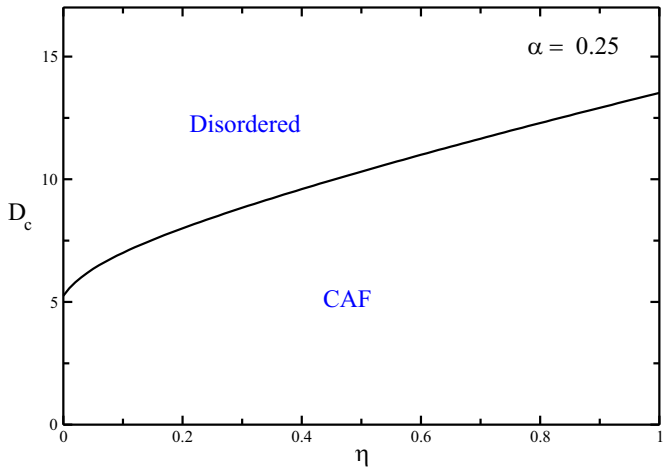

Fig. 4. Critical crystal field, D_c, as a function of the frustration parameter, $\eta > 0$, at zero temperature, for $\alpha = 0.25$.

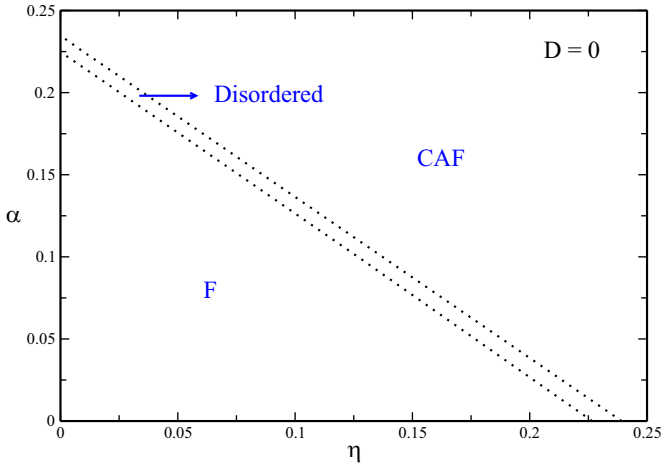

Fig. 6. α as a function of η, at zero temperature, for $D=0$. The dotted lines denote the first-order transitions between the ordered phase (F or CAF) and disordered one.

For $0 \le \alpha < 0.23$, the phase diagram is similar to the ones shown in Figs. 3 and 5. By contrast, for $\alpha \ge 0.23$, the phase diagram is modified, namely only the CAF phase is stabilized along the positive η-axis. A phase diagram in this range of frustration parameter is depicted in Fig. 4. Therefore the competition between J_1 and J_3 is responsible to suppress the ferromagnetic order for $\alpha \ge 0.23$, since J_3 frustrates the J_1 coupling. We remark that this feature is not observed in the corresponding model with both J_1 and J_3 antiferromagnetic, by reason of J_3 does not frustrate J_1, then, in this case, the Néel order is enhanced in contrast to the collinear one [16].

So far, we have only considered positive values of parameter η. However, if one allows negative values for J_2 coupling, which means that both J_1 and J_2 are ferromagnetic, the F phase will be stabilized along the negative η-axis even if $\alpha \ge 0.23$, as shown in Fig. 5. This happens because for $\eta < 0$, J_1 and J_2 does not compete with each other anymore, in contrast to the case depicted in Fig. 4, so that the F order increases as the parameter η becomes greater and negative. On the other hand, the CAF region becomes very thin, since, in this case, both J_1 and J_2 frustrates the antiferromagnetic coupling J_3 (see inset in Fig. 5).

For the sake of completeness, the phase diagram for $D=0$ is depicted in Fig. 6. We show the first-order phase transitions between the non-magnetic phase (disordered) and the ordered phase (F or CAF). As one can see, the disordered phase is very narrow and its width remains approximately constant as the frustration parameters are varied. In addition, we observe that both frustration parameters, α and η, have the same effect on the phase diagram: upon increasing α or η the phase transitions always occur from the ferromagnetic phase to the disordered phase, and then to the collinear phase.

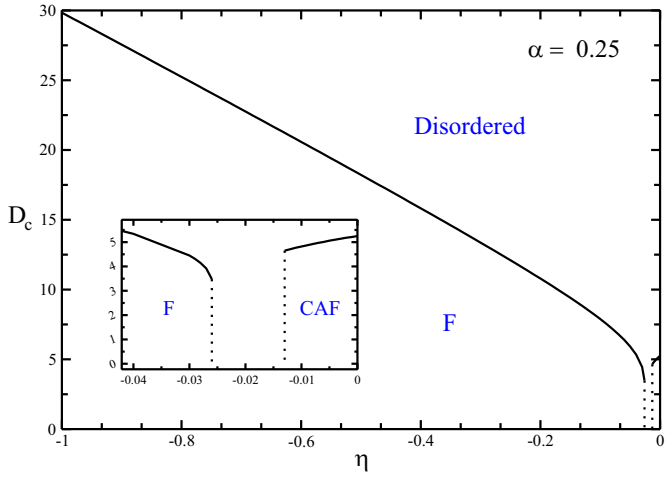

Fig. 5. Critical crystal field, D_c, as a function of the frustration parameter, $\eta < 0$, at zero temperature, for $\alpha = 0.25$. The continuous lines refer to second-order quantum phase transitions, and the dotted lines refer to first-order ones. The inset shows the low crystal field region on a finer scale.

3.2. Phase diagram at finite temperature

Up to now, we have set $T=0$. In this section, we turn our attention to the effect of temperature on the phase diagram of the present model. Thus, in contrast to the quantum phase transitions, the phase transitions analyzed here is driven by thermal fluctuations.

The behavior of the critical temperature, $T_c^{F(CAF)}$, as a function of the crystal field, for some values of η, is shown in Fig. 7. Phase transitions between the F phase and the disordered phase is depicted in Fig. 7(a) and (b) while the transitions between CAF phase and the disordered one is depicted in Fig. 7(c) and (d). A common feature is shared by all lines in Fig. 7: the critical temperature passes through a maximum upon increasing crystal field, and then decreases toward the quantum critical point. It should be mentioned that this is not a consequence of frustration, since unfrustrated Heisenberg model also exhibits it [17,26]. We believe that the quantum nature of the model, which is introduced by the non-commutativity of quantum mechanics spin operators, is responsible for this effect because in the classical Heisenberg model such characteristic is not observed: the critical temperature increases as the crystal field increases, and asymptotically approaches a constant value [27]. Consequently, in contrast to its quantum counterpart, the spins order down to absolute zero, even if the easy-plane anisotropy is very strong.

In Fig. 7(a) and (b), one notices that T_c^F decreases with increasing η, since the frustration weakens the ferromagnetic order, then less thermal fluctuations are required to drive the phase transition. By contrast, in Fig. 7(c) and (d), one can see that T_c^{CAF} increases as η increases because the collinear order is strengthened by the presence of J_2 coupling. We also conclude, by setting $\eta = 0.1$, that T_c^F is greater for $\alpha = 0$ (red full line in Fig. 7(a)) than for $\alpha = 0.1$ (blue dashed-dotted line in Fig. 7(b)). On the other hand, for $\eta = 0.4$ and $\eta = 1$, we observe that T_c^{CAF} is greater for $\alpha = 0.1$ (red full and black dashed lines in Fig. 7(d)) than for $\alpha = 0$ (red full and black dashed lines in Fig. 7(c)).

It seems worthwhile to analyze the behavior of the critical

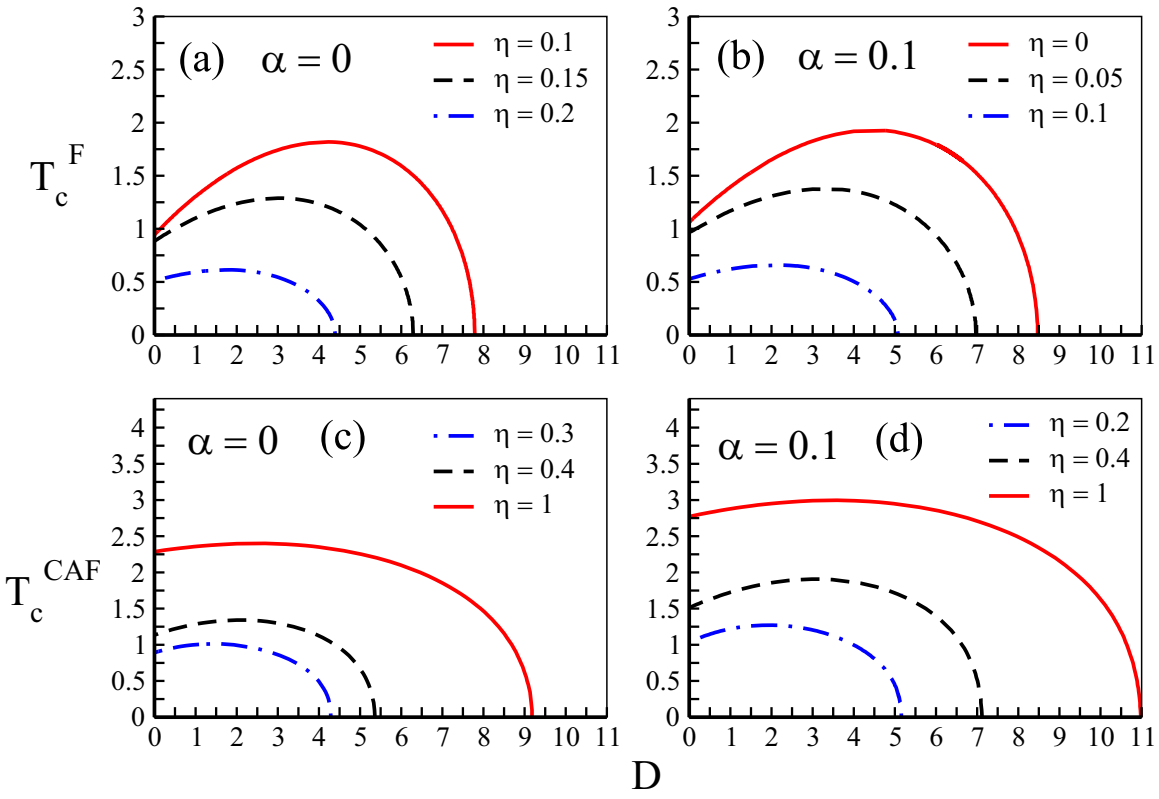

Fig. 7. Critical temperature, $T_c^{F(CAF)}$, as a function of the crystal field, D, for several values of frustration parameters, α and η. (For interpretation of the references to color in this figure caption, the reader is referred to the web version of this paper.)

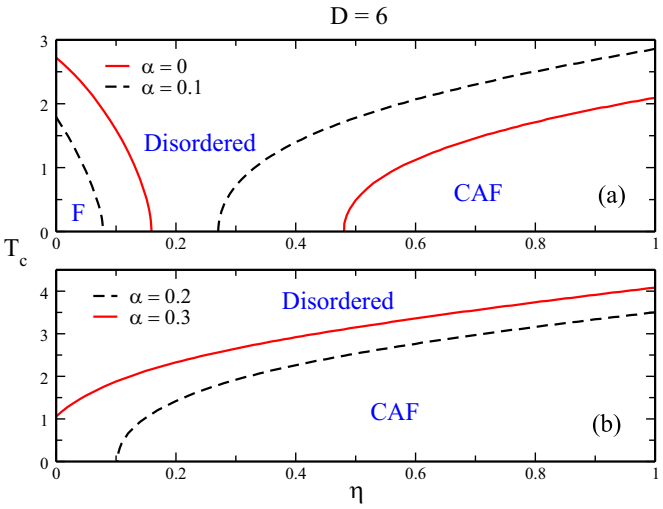

Fig. 8. Critical temperature, T_c, as a function of the frustration parameter, η, for some values of α.

temperature as a function of η for some values of α with $D \neq 0$. The results that are shown in Fig. 8(a) for $D=6$ indicate that the magnetically disordered region between F and CAF becomes smaller with increasing α. For $\alpha \geq 0.2$, as depicted in Fig. 8(b), the F phase is completely destroyed and the CAF region becomes larger. We would like to draw the attention of the reader to the disappearance of the F phase. This is a consequence of the range of parameter η: only positive values. As discussed in Section 3.1, by considering $\eta < 0$, J_1 and J_2 does not compete with each other, and then the ferromagnetic order will not disappear.

4. Concluding remarks

We have studied the spin-1 $J_1 - J_2 - J_3$ ferromagnetic Heisenberg model with an easy-plane crystal field on the cubic lattice by using the bond-operator formalism. Phase diagrams have been examined at finite and at zero temperatures. The zero-temperature phase diagrams exhibit a narrow magnetically disordered phase between the ferromagnetic and collinear antiferromagnetic phases for $D=0$ and $0 \leq \alpha < 0.23$. We suggest that such a disordered phase is a quantum spin liquid candidate. Second- and first-order phase transitions have been located according to the energy gap behavior. The effect of the crystal field, frustration and temperature on the stability of the ordered phases has also been analyzed in some cases.

One should mention that applications of numerical procedures to the present model would be very welcome in order to be compared with our analytical results, mainly to confirm the first-order transitions between the ordered and the disordered phases. Although, in general, numerical methods are not suitable to treat quantum systems in three dimensions, the variational cluster approach has been recently extended to study such systems [25], and then it can be used to verify the nature of these transitions.

As a final remark, the possibility of defining a nematic order induced by the crystal field ($D \neq 0$) at absolute zero in the present model will be subject of future investigation, since a nematic order has been found in its two-dimensional counterpart [4]. Furthermore, the extension of the present calculations to three-dimensional lattices with more complex geometries, such as hyperhoneycomb and stripyhoneycomb [10,12], deserves serious consideration.

Acknowledgments

The authors thank FAPEMIG (Fundação de Amparo à Pesquisa do Estado de Minas Gerais) and CNPq (Conselho Nacional de Desenvolvimento Científico e Tecnológico) for the financial support.

References

[1] P.W. Anderson, Mater. Res. Bull. 8 (1973) 153.
[2] L. Balents, Nature 464 (2010) 199.
[3] H. Feldner, D.C. Cabra, G.L. Rossini, Phys. Rev. B 84 (2011) 214406.
[4] A.S.T. Pires, Solid State Commun. 209 (2015) 18.
[5] J. Oitmaa, R.R.P. Singh, Phys. Rev. B 84 (2011) 094424.
[6] C. Waldtmann, et al., Eur. Phys. J. B 2 (1998) 501.
[7] T.P. Cysne, M.B. Silva Neto, arXiv:1504.01334v2, 2015.
[8] J. Richter, R. Darradi, J. Schulenburg, D.J.J. Farnell, H. Rosner, Phys. Rev. B 81 (2010) 174429.
[9] K. Majumdar, T. Datta, J. Stat. Phys. 139 (2010) 714.
[10] Y. Okamoto, M. Nohara, H. Aruga-Katori, H. Takagi, Phys. Rev. Lett. 99 (2007) 137207.
[11] I. Kimchi, J.G. Analytis, A. Vishwanath, Phys. Rev. B 90 (2014) 205126.
[12] T. Takayama, et al., Phys. Rev. Lett. 114 (2015) 077202.
[13] Z. Zhang, et al., Phys. Rev. B 87 (2013) 174405.
[14] J.G. Cheng, et al., Phys. Rev. Lett. 107 (2011) 197204.
[15] S. Bieri, et al., Phys. Rev. B 86 (2013) 224409.
[16] G.M.A. Sousa, A.S.T. Pires, Solid State Commun. 152 (2012) 1094.
[17] H-T. Wang, Y. Wang, Phys. Rev. B 71 (2005) 104429.
[18] A.S.T. Pires, J. Magn. Magn. Mater. 370 (2014) 106.
[19] M.A. Griffith, M.A. Continentino, A.S.T. Pires, J. Magn. Magn. Mater. (389) (2015) 61.
[20] A.S.T. Pires, Sol. State Commun. 217 (2015) 61.
[21] M. Troyer, U. Wiese, Phys. Rev. Lett. 94 (2005) 170201.
[22] S. Sachdev, R.N. Bhatt, Phys. Rev. B 41 (1990) 9323.
[23] H.-T. Wang, J.-L. Shen, Z.-B. Su, Phys. Rev. B 56 (1997) 14435.
[24] Xiao-Gang Wen, Quantum Field Theory of Many-Body Systems, Oxford Press, Oxford, 2004.
[25] M. Laubach, et al., Phys. Rev. B 93 (2016) 041106(R).
[26] D.C. Carvalho, J.A. Plascak, L.M. Castro, Phys. Rev. E 88 (2013) 032111.
[27] D.C. Carvalho, L.M. Castro, J.A. Plascak, Physica A 391 (2012) 1149.